

# ANALYTICAL STUDY OF THE TWO-DIMENSIONAL TIME-FRACTIONAL NAVIER-STOKES EQUATIONS\*

Jing Shao<sup>1,2,†</sup>, Boling Guo<sup>2</sup> and Lingling Duan<sup>1</sup>

**Abstract** In this paper, the two-dimensional (2D) Holf-Cole transformation with mass conservation in the frame of conformable derivative is developed, and then by introducing some exact solutions that satisfy linear differential equations and using the symbolic computation method, four exact solutions of 2D-nonlinear Navier-Stokes equations (NSEs) with the conformable time-fractional derivative are established. Some physical properties of the exact solutions are described preliminarily. Our results are the first ones on analytical study for the 2D time-fractional NSEs.

**Keywords** 2D Navier-Stokes equations, conformable fractional derivative, Holf-Cole transformation, exact solution.

**MSC(2010)** 76D05, 35B65.

## 1. Introduction

Nonlinear Navier-Stokes equations (NSEs) have been addressed extensively because of their demonstrated applications in hydromechanics, aeronautical sciences, meteorology, and other science branches. In recent literatures only a small number of exact solutions of the NSEs are reported, concerning the pulsating dean flow in a channel with porous walls, the steady flow in an annulus with porous wall, the stagnation flow on a plate with anisotropic slip and so on (see [10, 13, 15, 17, 18, 21, 22, 24, 25, 27] and references therein).

In this paper, we study the following two dimensional (2D)-nonlinear NSEs with the conformable time-fractional derivative

$$\mathbf{D}_t^\alpha \vec{u} + \vec{u} \cdot \nabla \vec{u} = -\nabla p + \nu \nabla^2 \vec{u}, \quad (1.1)$$

$$\nabla \cdot \vec{u} = 0, \quad (1.2)$$

where  $\mathbf{D}_t^\alpha(\cdot)$  is the conformable fractional derivative,  $0 < \alpha \leq 1$ ,  $\vec{u} = \vec{u}(t, x, y)$ ,  $p = p(t, x, y)$ ,  $\nu$  and  $\nabla$  are the fluid velocity field, the fluid pressure, the viscosity

---

<sup>†</sup>the corresponding author. Email address: shaojing99500@163.com(J. Shao)

<sup>1</sup>Department of Mathematics, Jining University, No.1 Xingtian Road, Qufu 273155, Shandong, China

<sup>2</sup>Institute of Applied Physics and Computational Mathematics, No.6 Huayuan Road, Beijing 100088, China

\*Project supported by NNSF of China (Nos 11671227 and 11271225), NSF of Shandong (No ZR2018LA004), and Science and Technology Project of High Schools of Shandong (Nos J18KA220, J18KB107).

and the gradient, respectively. The variables  $x$  and  $y$  form a Cartesian coordinate system;  $u_1, u_2$  are the components of  $\vec{u}$ .

Notice that the problem (1.1) reduces to the classical NSEs for  $\alpha = 1$ :

$$\vec{u}_t + \vec{u} \cdot \nabla \vec{u} = -\nabla p + \nu \nabla^2 \vec{u}. \quad (1.3)$$

In 1977, Takeo Saitoh [15] considered the full NSEs (1.3) by a numerical scheme with a high degree of accuracy. A fortunate exact solution was produced for flow in a porous pipe in [18]. By Chebyshev expansion methods, H. C. Ku et al. [10] studied the solutions of the steady 2D-NSEs in both the vorticity-stream function and the vorticity-velocity formulation. In 1998, G. Profilo et al. [13] solved the 2D-NSEs by the symmetry approach. The pseudo-spectral solutions of the 2D incompressible NSEs on a disk with no-slip boundary conditions were studied in [21]. The analyticity of solutions for randomly forced 2D-NSEs with periodic boundary conditions were discussed in [17]. By similarity transform, C. Y. Wang [24] investigated the flow due to a stretching flat boundary with partial slip. Analytical solutions of the equations of motion of a Newtonian fluid for the fully developed laminar flow between two concentric cylinders were presented by S. Tsangaris in the literature [22]. The numerical methods for solving the 2D-NSEs have been investigated by authors [3, 6–8, 16, 26].

Fractional calculus has attracted much attention from mathematicians, physicists, biology, chemistry, engineering and other areas of applications in recent decades. Various types of definitions of fractional derivative are given, such as Grünwald-Letnikov, Riemann-Liouville and Caputo's fractional derivatives [5, 12]. Most of them are defined via fractional integrals, thus they have nonlocal properties. The theory of conformable fractional calculus is a new topic of research which is introduced by Khalil et al. [9] in 2014. This new fractional derivative is a well-behaved definition, which depends on the basic limit definition of the derivative, and has governed much attention in recent years. In 2015, Abdeljawad studied fractional versions of the chain rule, exponential functions, Gronwall inequality, integration by parts (see [1] for details). Atangana et al. [2] investigated some new properties of this derivative, such as Taylor power series expansions, the conformable partial derivative, the conformable gradient, the conformable divergence theorem, and so on. The fractional Newtonian mechanics and the fractional version of the calculus of variations were introduced, and the fractional Euler-Lagrange equation was constructed in [4]. D. Zhao and M. Luo [28] generalized the conformable derivative and gave the physical and geometrical interpretation of generalized conformable derivative in 2017.

There is a considerable interest in the study of time fractional Navier-Stokes equations (TFNSEs). Most of them are 1D-TFNSEs. There are also some analytical methods available for solving the TFNSEs. The homotopy analysis method is used to obtain an approximate solution of the nonlinear 1D-TFNSEs by introducing the Caputo's fractional derivative, see Ragab, Hemida, Mohamed and Salam [14]. In [29], Y. Zhou and L. Peng established the existence criterion of weak solutions of the 1D-TFNSEs by means of Galerkin approximations in the case that the dimension  $n \leq 4$ , which can be used to simulate anomalous diffusion in fractal media. Moreover, L. Peng, A. Debbouche and Y. Zhou investigated the existence and Faedo-Galerkin approximations of solutions for 1D-TFNSEs with Caputo derivative operators in the paper [11]. In 2018, G. Zou et al. [30] solved the numerical solution of 1D-TFNSEs by applying a composite idea of semi-discrete finite difference

approximation in time and Galerkin finite element method in space with Caputo derivative of order  $0 < \alpha < 1$ .

However, to our best knowledge, there is no result on the exact solution of the 2D-TFNSEs, especially result with conformable fractional derivative operator. In 2007, C. Wu et al. [23] considered the following 2D-NSEs

$$\begin{cases} u_t + uu_x + vv_y + p_x = \frac{1}{Re} (u_{xx} + u_{yy}), \\ v_t + uv_x + vv_y + p_y = \frac{1}{Re} (v_{xx} + v_{yy}), \end{cases}$$

and the continuity equation is

$$u_x + v_y = 0,$$

where  $x$  and  $y$  form a Cartesian coordinate system; the variables  $u$  and  $v$  are the components of the fluid vector  $\vec{V}$  in the  $x$  and  $y$  directions, respectively;  $Re$  is Reynolds number; variable  $p$  is the fluid pressure;  $u_t \triangleq \frac{\partial u(t,x,y)}{\partial t}$ ,  $u_{xx} \triangleq \frac{\partial^2 u(t,x,y)}{\partial x^2}$ . Three exact solutions of the 2D-NSEs are presented by using the method of 2D Hopf-Cole transformation with mass conservation.

Followed the above references, the main contribution of our paper is to provide some exact solutions of 2D-TFNSEs in the frame of conformable derivative and to discuss some interesting physical properties of these exact solutions. The rest of the paper is arranged as follows. In section 2, we give some definitions, properties of conformable fractional operators and the procedure of the Jacobi elliptic function expansion method. In section 3, the 2D Holf-Cole transformation with mass conservation in the frame of conformable derivative is developed. And then in section 4, by introducing some 2D exact solutions that satisfy linear differential equations and using the symbolic computation method in Refs. [19], [20], four exact solutions of 2D-TFNSEs are established. In order to reveal some relevant physical aspects of the obtained results, some figures are presented for various parameters by using the analytical solutions obtained in section 3. In section 5, we give some comments on our paper.

## 2. Basic definitions and tools

To address our main result, here we represent the definitions, symbols and known properties of conformable fractional operators which will be used in the remainder of this paper.

**Definition 2.1.** The (left) conformable fractional derivative starting from  $t_0$  of a function  $f : [t_0, \infty) \rightarrow \mathbb{R}$  of order  $\alpha$  with  $0 < \alpha \leq 1$  is defined by

$$({}_{t_0}\mathbf{D}_t^\alpha f)(t) = \lim_{\varepsilon \rightarrow 0} \frac{f(t + \varepsilon(t - t_0)^{1-\alpha}) - f(t)}{\varepsilon}.$$

If  $({}_{t_0}\mathbf{D}_t^\alpha f)(t)$  exists at  $t \geq t_0$ , we say  $f$  is  $\alpha$ -differentiable at point  $t$ , and if  $({}_{t_0}\mathbf{D}_t^\alpha f)(t)$  exists on  $(t_0, t_1)$ , then  $({}_{t_0}\mathbf{D}_t^\alpha f)(t_0) = \lim_{t \rightarrow t_0^+} ({}_{t_0}\mathbf{D}_t^\alpha f)(t)$ .

**Definition 2.2.** Let  $\alpha \in (0, 1]$ . The left conformable fractional integral of order  $\alpha$  starting at  $t_0$  is defined by

$$({}_{t_0}\mathbf{I}_t^\alpha f)(t) = \int_{t_0}^t (x - t_0)^{\alpha-1} f(x) dx.$$

If  $t_0 = 0$ ,  $\mathbf{D}_t^\alpha f \triangleq ({}_{t_0}\mathbf{D}_t^\alpha f)(t)$ ,  $\mathbf{I}_t^\alpha f \triangleq ({}_{t_0}\mathbf{I}_t^\alpha f)(t)$ . We note that for  $\alpha \in (0, 1]$ , the definition of conformable fractional integral is the same as Riemann-Liouville fractional integral up to a constant multiplier.

In the higher order case, we can generalize to the following definitions.

**Definition 2.3.** Let  $\alpha \in (n, n + 1]$ . The (left) conformable fractional derivative starting from  $t_0$  of a function  $f : [t_0, \infty) \rightarrow \mathbb{R}$  of order  $\alpha$ , where  $f^{(n)}(t)$  exists, is defined by

$$({}_{t_0}\mathbf{D}_t^\alpha f)(t) = \left( {}_{t_0}\mathbf{D}_t^{\alpha-n} f^{(n)} \right) (t).$$

**Definition 2.4.** Let  $\alpha \in (n, n + 1]$ . The (left) conformable fractional integral of order  $\alpha$  starting at  $t_0$  is defined by

$$({}_{t_0}\mathbf{I}_t^\alpha f)(t) = {}_{t_0}\mathbf{I}_t^{n+1} \left( (t-t_0)^{\alpha-n-1} f \right) (t) = \frac{1}{n!} \int_{t_0}^t (t-x)^n (x-t_0)^{\alpha-n-1} f(x) dx.$$

**Lemma 2.1** (see [9]). If  $\alpha \in (n, n + 1]$  and  $f : [t_0, \infty) \rightarrow \mathbb{R}$  is an  $(n + 1)$  times differentiable function for  $t > t_0$ . Then, for all  $t > t_0$ , we have

$${}_{t_0}\mathbf{I}_t^\alpha {}_{t_0}\mathbf{D}_t^\alpha (f)(t) = f(t) - \sum_{k=0}^n \frac{f^{(k)}(t_0)(t-t_0)^k}{k!}. \quad (2.1)$$

**Lemma 2.2** (see [1]). Let  $\alpha \in (0, 1]$  and suppose  $f, g$  are  $\alpha$ -differentiable at point  $t > 0$ . Then

1.  ${}_{t_0}\mathbf{D}_t^\alpha (af + bg) = a \cdot {}_{t_0}\mathbf{D}_t^\alpha (f) + b \cdot {}_{t_0}\mathbf{D}_t^\alpha (g)$  for all real constant  $a, b$ ;
2.  ${}_{t_0}\mathbf{D}_t^\alpha (fg) = f \cdot {}_{t_0}\mathbf{D}_t^\alpha (g) + g \cdot {}_{t_0}\mathbf{D}_t^\alpha (f)$ ;
3.  ${}_{t_0}\mathbf{D}_t^\alpha (t^p) = pt^{p-\alpha}$ , for all  $p$ ;
4.  ${}_{t_0}\mathbf{D}_t^\alpha \left( \frac{f}{g} \right) = \frac{g \cdot {}_{t_0}\mathbf{D}_t^\alpha (f) - f \cdot {}_{t_0}\mathbf{D}_t^\alpha (g)}{g^2}$ ;
5.  ${}_{t_0}\mathbf{D}_t^\alpha (c) = 0$ , where  $c$  is a constant;
6.  $({}_{t_0}\mathbf{D}_t^\alpha f)(t) = (t-t_0)^{1-\alpha} f'(t)$ .

Now we describe the procedure of the Jacobi elliptic function expansion method. Given a nonlinear wave equation

$$F \left( u, \mathbf{D}_t^\alpha u, \frac{\partial u}{\partial x}, \frac{\partial u}{\partial y}, \mathbf{D}_t^{2\alpha} u, \frac{\partial^2 u}{\partial x^2}, \frac{\partial^2 u}{\partial y^2}, \dots \right) = 0, \quad (2.2)$$

where  $\mathbf{D}_t^{n\alpha}(\cdot) = \underbrace{\mathbf{D}_t^\alpha \cdots \mathbf{D}_t^\alpha}_{n}(\cdot)$ ,  $n \in \mathbb{N}$ . Transforming (2.2), applying the chain rule [1] and letting  $t_0 = 0$ ,

$$u = u(\xi), \xi = l \frac{t^\alpha}{\alpha} + mx + ny,$$

where  $l, m$ , and  $n$  are arbitrary constants,

$$\mathbf{D}_t^\alpha(\cdot) = l \frac{d(\cdot)}{d\xi}, \frac{\partial(\cdot)}{\partial x} = m \frac{d(\cdot)}{d\xi}, \frac{\partial(\cdot)}{\partial y} = n \frac{d(\cdot)}{d\xi}, \dots \quad (2.3)$$

yields an ordinary differential equation (ODE) for  $u(\xi)$ ,

$$O(u, u', u'', u''', \dots),$$

where the prime denotes the derivative with respect to  $\xi$ .

**Example 2.1. 2D conformable time fractional heat-conduction equation.**

Using the Jacobi elliptic function expansion method, let us consider the conformable time-fractional heat conduction equation

$$\mathbf{D}_t^\alpha W(t, x, y) = \nu (W_{xx} + W_{yy}).$$

Suppose that  $W(t, x, y) = W(\xi)$ ,  $\xi = x + y - l \frac{t^\alpha}{\alpha}$ , where  $l$  is constant, we get

$$W_{\xi\xi} + \frac{l}{2\nu} W_\xi = 0. \quad (2.4)$$

It is easy to get a simple solution of (2.4). That is

$$W(\xi) = \frac{2C\nu}{l} + C^* \exp \left\{ -\frac{l}{2\nu} \xi \right\},$$

where  $C$  and  $C^*$  are constants. Hence we get

$$W(t, x, y) = \frac{2C\nu}{l} + C^* \exp \left\{ -\frac{l}{2\nu} \left( x + y - l \frac{t^\alpha}{\alpha} \right) \right\}.$$

### 3. 2D Hopf-Cole transformation with mass conservation

#### 3.1. Expression of 2D Hopf-Cole transformation

The conformable nonlinear 2D-TFNSEs is of the form

$$\begin{cases} \mathbf{D}_t^\alpha u_1 + u_1 u_{1x} + u_2 u_{1y} + p_x = \nu (u_{1xx} + u_{1yy}), \\ \mathbf{D}_t^\alpha u_2 + u_1 u_{2x} + u_2 u_{2y} + p_y = \nu (u_{2xx} + u_{2yy}), \end{cases} \quad (3.1)$$

and

$$u_{1x} + u_{2y} = 0. \quad (3.2)$$

We recall that the stream function  $\psi$  is defined by

$$u_1 = -\frac{\partial \psi}{\partial y}, u_2 = \frac{\partial \psi}{\partial x}. \quad (3.3)$$

Substituting (3.3) into (3.2), we get

$$\begin{aligned} u_1 u_{1x} + u_2 u_{1y} &= -(\psi_x \psi_y)_y + (\psi_y^2)_x, \\ u_1 u_{2x} + u_2 u_{2y} &= -(\psi_x \psi_y)_x + (\psi_x^2)_y. \end{aligned} \quad (3.4)$$

Using (3.3) and (3.4) in (3.1), we have

$$\begin{aligned} - \left[ \mathbf{D}_t^\alpha \psi + \frac{1}{2} (\psi_x^2 + \psi_y^2) - \nu (\psi_{xx} + \psi_{yy}) \right]_y + \frac{1}{2} [(\psi_x - \psi_y)^2]_y + p_x + (\psi_y^2)_x &= 0, \\ \left[ \mathbf{D}_t^\alpha \psi + \frac{1}{2} (\psi_x^2 + \psi_y^2) - \nu (\psi_{xx} + \psi_{yy}) \right]_x - \frac{1}{2} [(\psi_x + \psi_y)^2]_x + p_y + (\psi_x^2)_y &= 0. \end{aligned} \quad (3.5)$$

Letting

$$\begin{aligned} p_x &= -\frac{1}{2} \left[ (\psi_x - \psi_y)^2 \right]_y - (\psi_y^2)_x, \\ p_y &= \frac{1}{2} \left[ (\psi_x + \psi_y)^2 \right]_x - (\psi_x^2)_y, \end{aligned} \quad (3.6)$$

and the integral constant being zero, we get the following simple expression via performing integration for  $x$  and  $y$  directions,

$$\mathbf{D}_t^\alpha \psi + \frac{1}{2} (\psi_x^2 + \psi_y^2) - \nu (\psi_{xx} + \psi_{yy}) = 0. \quad (3.7)$$

We introduce a variable  $W$  now which satisfies the following linear differential equation

$$\mathbf{D}_t^\alpha W - \nu (W_{xx} + W_{yy}) = 0, \quad (3.8)$$

and we assume that

$$W = W(t, x, y) = F(\psi), \quad (3.9)$$

then we can structure a transformation between variables  $F$  and  $\psi$ . Substituting (3.9) into (3.8) and using Lemma 2.2, we have

$$\mathbf{D}_t^\alpha \psi - \frac{\nu F_{\psi\psi}}{F_\psi} (\psi_x^2 + \psi_y^2) - \nu (\psi_{xx} + \psi_{yy}) = 0. \quad (3.10)$$

Comparing (3.7) with (3.10), we can see that there is a relation

$$-\frac{1}{2} = \nu \frac{F_{\psi\psi}}{F_\psi}. \quad (3.11)$$

Making all integral constants being zero in the course of solving (3.11), then the following transformation between variables  $F$  and  $\psi$  can be obtained

$$\psi = -2\nu \ln \left( -\frac{1}{2\nu} W \right). \quad (3.12)$$

Substituting (3.12) into (3.3) and (3.7), we get

$$u_1 = 2\nu \frac{W_y}{W}, u_2 = -2\nu \frac{W_x}{W}; \quad (3.13)$$

$$\begin{aligned} p_x &= -2\nu^2 \left( \frac{(W_y - W_x)^2}{W^2} \right)_y - 4\nu^2 \left( \frac{W_y^2}{W^2} \right)_x \\ &= -\frac{1}{2} [(u_1 + u_2)^2]_y - (u_1^2)_x, \\ p_y &= 2\nu^2 \left( \frac{(W_x + W_y)^2}{W^2} \right)_x - 4\nu^2 \left( \frac{W_x^2}{W^2} \right)_y \\ &= \frac{1}{2} [(u_2 - u_1)^2]_x - (u_2^2)_y. \end{aligned} \quad (3.14)$$

Furthermore,  $W$  can be solved in (3.8), and then  $u_1$ ,  $u_2$  and  $p_x$ ,  $p_y$  can be obtained via solving (3.13) ~ (3.14). Substituting  $u_1$ ,  $u_2$  and  $p_x$ ,  $p_y$  into (3.1) ~ (3.2), we get

$$\begin{aligned} &2\nu \mathbf{D}_t^\alpha (\ln F_\psi)_y + 4\nu^2 (\ln F_\psi)_y (\ln F_\psi)_{yx} + 4\nu^2 (\ln F_\psi)_x (\ln F_\psi)_{xy} + p_x \\ &= 2\nu^2 (\ln F_\psi)_{yxx} + 2\nu^2 (\ln F_\psi)_{yyy}, \end{aligned}$$

$$\begin{aligned} & 2\nu \mathbf{D}_t^\alpha (\ln F_\psi)_x + 4\nu^2 (\ln F_\psi)_y (\ln F_\psi)_{xx} - 4\nu^2 (\ln F_\psi)_x (\ln F_\psi)_{xy} + p_y \\ & = 2\nu^2 (\ln F_\psi)_{xxx} + 2\nu^2 (\ln F_\psi)_{xyy}. \end{aligned}$$

Using the symbolic computation method in Refs. [19], [20] to calculate these variables, we know that  $u_1$ ,  $u_2$  and  $p_x$ ,  $p_y$  satisfy (3.1) ~ (3.2). Thus (3.13) ~ (3.14) make up a 2D Hopf-Cole transformation of the conformable nonlinear 2D-TFNSEs.

If  $u_1$ ,  $u_2$  and  $p_x$ ,  $p_y$  are structured by using some trigonometric functions and exponential functions as in section 4 case 4, then  $p_x$  and  $p_y$  do not satisfy (3.14). In this case,  $u_1$  and  $u_2$  have been obtained by (3.13) under the precondition that  $W$  satisfies (3.8), and then  $p_x$  and  $p_y$  can be obtained by the following equations

$$\begin{aligned} p_x &= \nu (u_{1xx} + u_{1yy}) - \mathbf{D}_t^\alpha u_1 - u_1 u_{1x} - u_2 u_{1y}, \\ p_y &= \nu (u_{2xx} + u_{2yy}) - \mathbf{D}_t^\alpha u_2 - u_1 u_{2x} - u_2 u_{2y}. \end{aligned} \quad (3.15)$$

### 3.2. Modified expression of 2D Hopf-Cole transformation

Followed the procedure of 2D Hopf-Cole transformation, we obtain (3.4) ~ (3.7). Introducing a new variable  $V$  that satisfies the following linear differential equation

$$\mathbf{D}_t^\alpha V + h(t, x, y) - \nu (V_{xx} + V_{yy}) = 0, \quad (3.16)$$

and assuming

$$V = C_0 + V_1(t)H(t, x, y) = C_0 + V_1(t)H(\psi), \quad (3.17)$$

here  $h(t, x, y)$  may be structured as follows

$$h(t, x, y) = -\mathbf{D}_t^\alpha (V_1(t)) H(t, x, y), \quad (3.18)$$

where  $V_1(t)$  is a point source varying with time and  $C_0$  is a constant.

Using the similar discussion as 2D Hopf-Cole transformation, we can obtain a modified expression of 2D Hopf-Cole transformation with mass conservation as follows

$$\begin{aligned} \psi &= -2\nu \ln \left( -\frac{1}{2\nu} V \right); \\ u_1 &= 2\nu \frac{V_y}{V}, u_2 = -2\nu \frac{V_x}{V}; \\ p_x &= -2\nu^2 \left( \frac{(W_y - W_x)^2}{W^2} \right)_y - 4\nu^2 \left( \frac{W_y^2}{W^2} \right)_x + A_1 \\ &= -\frac{1}{2} \left[ (u_1 + u_2)^2 \right]_y - (u_1^2)_x + A_1, \\ p_y &= 2\nu^2 \left( \frac{(W_x + W_y)^2}{W^2} \right)_x - 4\nu^2 \left( \frac{W_x^2}{W^2} \right)_y + A_2 \\ &= \frac{1}{2} \left[ (u_2 - u_1)^2 \right]_x - (u_2^2)_y + A_2, \end{aligned} \quad (3.19)$$

where

$$A_1 = -\mathbf{D}_t^\alpha [V_1(t)] \cdot \frac{u_1}{V_1(t)V(t)} \quad (3.20)$$

and

$$A_2 = -\mathbf{D}_t^\alpha [V_1(t)] \cdot \frac{u_2}{V_1(t)V(t)}. \quad (3.21)$$

If  $V_1(t) = 1$  in (3.17), then (3.17) reduces to (3.9). By the symbolic computation method, we learn that  $H(t, x, y)$  is the same as the solution of  $W(t, x, y)$ , and  $V_1(t)$  is a differentiable function,  $h(t, x, y)$  can structure the  $V(x, y, t)$  that satisfies (3.16).

If the point source is a constant, then  $A_1$  and  $A_2$  are zeros in (3.20) and (3.21), thus (3.19) reduces to (3.13) and (3.14).

### 3.3. Properties of $p_x$ and $p_y$

Note that since some exact solutions of 2D-NSEs in this paper are vortex solutions, they can be expressed in two orthogonal coordinate systems reciprocally. We introduce a new coordinate system  $(X, Y)$  and two new variables  $U_1$  and  $U_2$  which are defined by

$$x = -Y, y = X, u_1 = -U_2, u_2 = U_1. \quad (3.22)$$

Under the new coordinate system (3.22), the expressions in (3.19) are changed into

$$\begin{aligned} p_Y &= \frac{1}{2} \left[ (U_2 - U_1)^2 \right]_X - (U_2^2)_Y - \mathbf{D}_t^\alpha [V_1(t)] \cdot \frac{U_2}{V_1(t)V(t)}, \\ p_X &= -\frac{1}{2} \left[ (U_1 + U_2)^2 \right]_Y - (U_1^2)_X - \mathbf{D}_t^\alpha [V_1(t)] \cdot \frac{U_1}{V_1(t)V(t)}. \end{aligned} \quad (3.23)$$

Substituting (3.22) into (3.15), we get

$$\begin{aligned} p_Y &= \nu (U_{2XX} + U_{2YY}) - \mathbf{D}_t^\alpha U_2 - U_1 U_{2X} - U_2 U_{2Y}, \\ p_X &= \nu (U_{1XX} + U_{1YY}) - \mathbf{D}_t^\alpha U_1 - U_1 U_{1X} - U_2 U_{1Y}. \end{aligned} \quad (3.24)$$

Comparing (3.23), (3.24) with (3.19), (3.15), we get the following conclusions.

- (i) The expressions of  $p_x, p_y$  and  $p_X, p_Y$  will be exchanged reciprocally.
- (ii)  $p_x$  and  $p_y$  are orthogonal symmetry reciprocally, and

$$\begin{aligned} \int p_x dx &= p(u_1, u_2, x, y, t), \\ \int p_y dy &= \int p_X dX = p(U_1, U_2, X, Y, t). \end{aligned} \quad (3.25)$$

- (iii)  $p(u_1, u_2, x, y, t) = p(U_1, U_2, X, Y, t)$ .

(iv) The fluid velocity field  $\vec{u}$ , the fluid pressure  $p$  in some vortex solutions are orthogonal symmetric distribution for origin ( $x = 0, y = 0$ ), thus  $p_x$  and  $p_y$  are compatible to each other.

## 4. Statement of the problem and its exact solutions on infinity plane

In this section, we consider some exact solutions of 2D-TFNSEs in many cases.

### Case 1. An exact solution on infinity plane

Introducing an exact solution that satisfies (3.8) of the form

$$W(t, x, y) = \frac{2C\nu}{l} + C^* E_1 \quad (4.1)$$

and substituting (4.1) into (3.12)  $\sim$  (3.14), we have

$$\begin{aligned}\psi &= -2\nu \ln \left( -\frac{C}{l} - C^* E_1 \right), C < 0, C^* < 0; \\ u_1 &= \frac{-C^* l^2 E_1}{C + l C^* E_1}, u_2 = \frac{C^* l^2 E_1}{C + l C^* E_1}; \\ p_x &= \frac{C^{*2} C l^5 E_1^2}{\nu(C + l C^* E_1)^3}, p_y = \frac{\nu C C^{*2} l^5 E_1^2 - 2 C^{*2} C l^5 E_1^4}{\nu(C + l C^* E_1)^3},\end{aligned}\quad (4.2)$$

where  $\psi$  is the stream function and  $E_1 = e^{-\frac{l}{2\nu}(x+y-l\frac{t^\alpha}{\alpha})}$ . Substituting  $u_1$ ,  $u_2$  and  $p_x$ ,  $p_y$  into (3.1)  $\sim$  (3.2) and using the symbolic computation method to calculate these variables, respectively, we can learn that the variables satisfy (3.1)  $\sim$  (3.2). Hence  $u_1$ ,  $u_2$  and  $p_x$ ,  $p_y$  in (4.2) constitute an exact solution of conformable time-fractional 2D-NSEs.

In the first case, the coefficients of (4.2) are  $\nu = 0.1$ ,  $l = 1$ ,  $C = -1$ ,  $C^* = -2$ . Then we can find some interesting physical behaviour of this exact solution with the fractional order  $\alpha = \frac{1}{2}$  at the time  $t = 1$ ,  $t = 10$  and  $t = 100$ , as shown in Figs. 1, 2 and 3.

(i) From Fig. 1, we see that the vectorial distribution of the fluid velocity vector  $\vec{u}$  is strip region and it is increasing as  $t$  increasing. The flown line distribution of  $\vec{u}$  is a series of parallel lines. Particularly, the flown line distribution of  $\vec{u}$  in the region  $X \times Y \in [-20, 20] \times [-20, 20]$ , the flown line distribution of  $\vec{u}$  is more intensive than in the rest of the region.

(ii) Fig. 2 shows that the surface distribution of  $u_1$  and  $u_2$  change with  $\alpha = \frac{1}{2}$  at the time  $t = 1$ ,  $t = 10$ , and  $t = 100$ . It can be seen clearly that the valued field of  $u_1$  is  $[-1, 0]$  and the surface distribution of  $u_1$  decreases gradually to  $u_1 = 1$  as the increasing of  $t$ . And then the valued field of  $u_2$  is  $[0, 1]$  and the surface distribution of  $u_2$  increases gradually to  $u_2 = 1$  with the increasing of  $t$ .

(iii) Fig. 3 depicts the surface distribution of  $p_x$  and  $p_y$  for three different values of  $t$ . It is clear that the surface distribution of  $p_x$  decreases from  $+\infty$  to 0, and the surface distribution of  $p_y$  increases from  $-\infty$  to 0. Hence we get that as time goes on, the surface distribution of  $p_x$  and  $p_y$  will be on the plane  $p_x = 0$  and  $p_y = 0$  eventually.

## Case 2. An exact solution under action of a point source on infinity plane

Introducing an exact solution that satisfies (3.8) of the form

$$W(t, x, y) = 1 + \frac{a_0}{4\pi\nu t^\alpha} E_2 \quad (4.3)$$

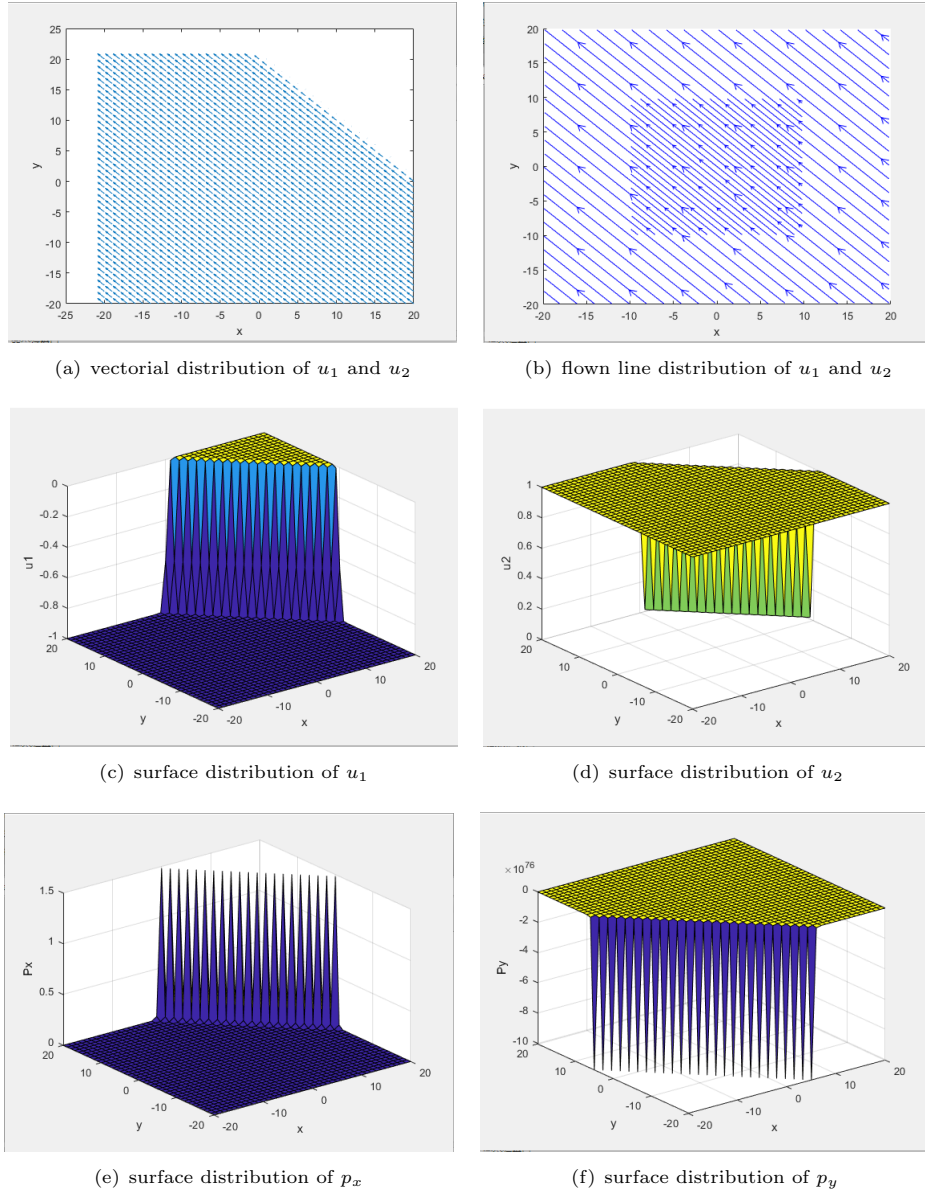


**Figure 1.** Case 1. The parameters are chosen as:  $\nu = 0.1$ ,  $l = 1$ ,  $t = 10$ ,  $C = -1$ ,  $C^* = -2$  and  $\alpha = \frac{1}{2}$ .

and substituting (4.3) into (3.12) ~ (3.14), we have

$$\begin{aligned}
 \psi &= -2\nu \ln \left( -\frac{1}{2\nu} - \frac{a_0}{8\pi\nu^2 t^\alpha} E_2 \right); \\
 u_1 &= \frac{-ya_0\alpha E_2}{4\pi\nu t^{2\alpha} + a_0 t^\alpha E_2}, u_2 = \frac{xa_0\alpha E_2}{4\pi\nu t^{2\alpha} + a_0 t^\alpha E_2}; \\
 p_x &= \frac{a_0^2 \alpha^2 E_2^2}{(4\pi\nu t^{2\alpha} + a_0 t^\alpha E_2)^3} \\
 &\quad \cdot [4\pi\alpha xy^2 t^\alpha - 4\pi\nu(y-x)t^{2\alpha} - a_0(y-x)t^\alpha E_2 - 2\pi\alpha y(x-y)^2 t^\alpha], \\
 p_y &= \frac{a_0^2 \alpha^2 E_2^2}{(4\pi\nu t^{2\alpha} + a_0 t^\alpha E_2)^3} \\
 &\quad \cdot [4\pi\alpha x^2 y t^\alpha + 4\pi\nu(x+y)t^{2\alpha} + a_0(x+y)t^\alpha E_2 - 2\pi\alpha x(x+y)^2 t^\alpha],
 \end{aligned} \tag{4.4}$$

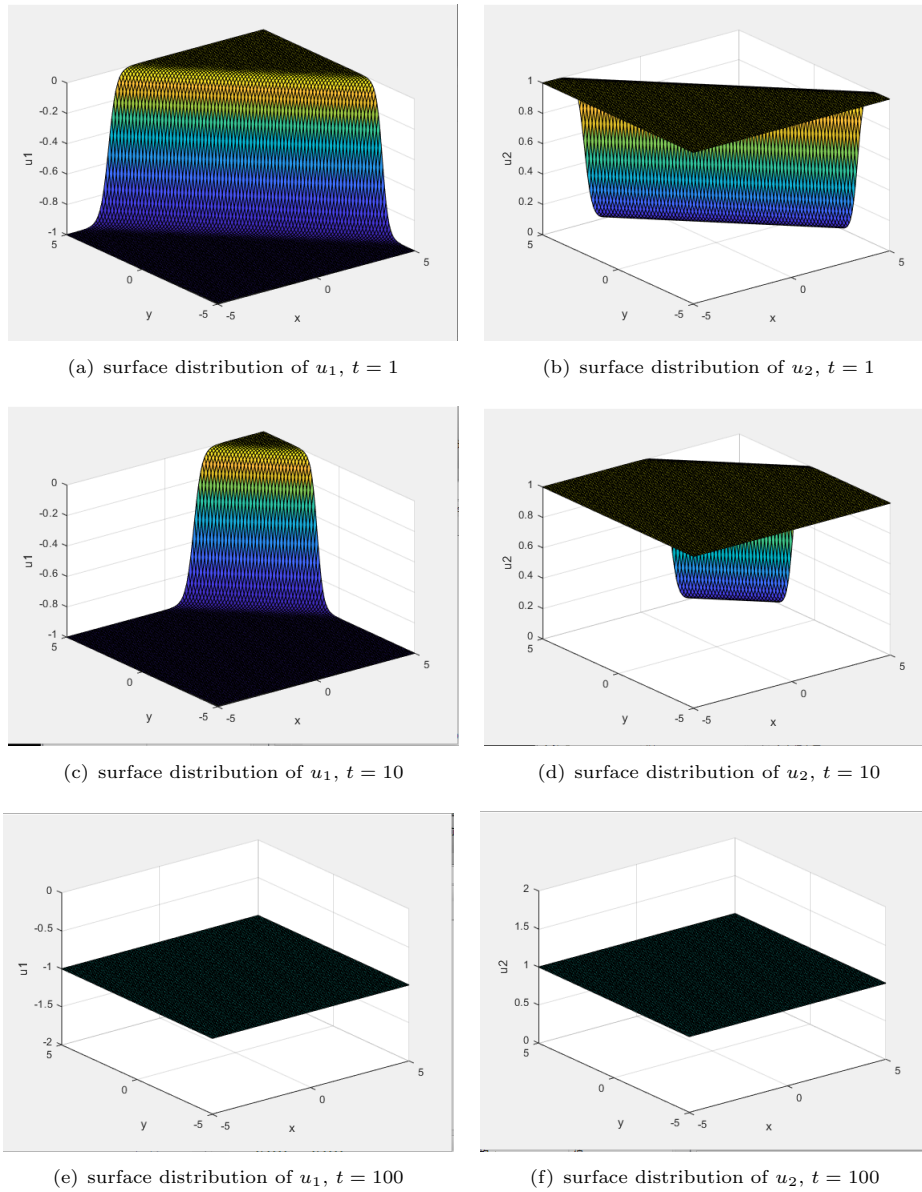


**Figure 2.** Case 1. The parameters are chosen as:  $\nu = 0.1$ ,  $l = 1$ ,  $C = -1$ ,  $C^* = -2$  and  $\alpha = \frac{1}{2}$ .

where  $\psi$  is the stream function and  $E_2 = \exp\left\{-\frac{\alpha(x^2+y^2)}{4t^{\alpha\nu}}\right\}$ . Following the procedure of the first case, we conclude that  $u_1$ ,  $u_2$  and  $p_x$ ,  $p_y$  in (4.4) constitute an exact solution of conformable TFNSEs.

In the second case, the parameters are chosen as:  $\nu = 0.1$ ,  $a_0 = \exp(1)$  with the fractional parameter  $\alpha = \frac{1}{2}$  at the time  $t = 1$ ,  $t = 10$ ,  $t = 100$  and  $t = 10000$ , respectively. Then we can find some physical behaviors of this exact solution, as shown in Figs. 4, 5, 6, 7, and 8.

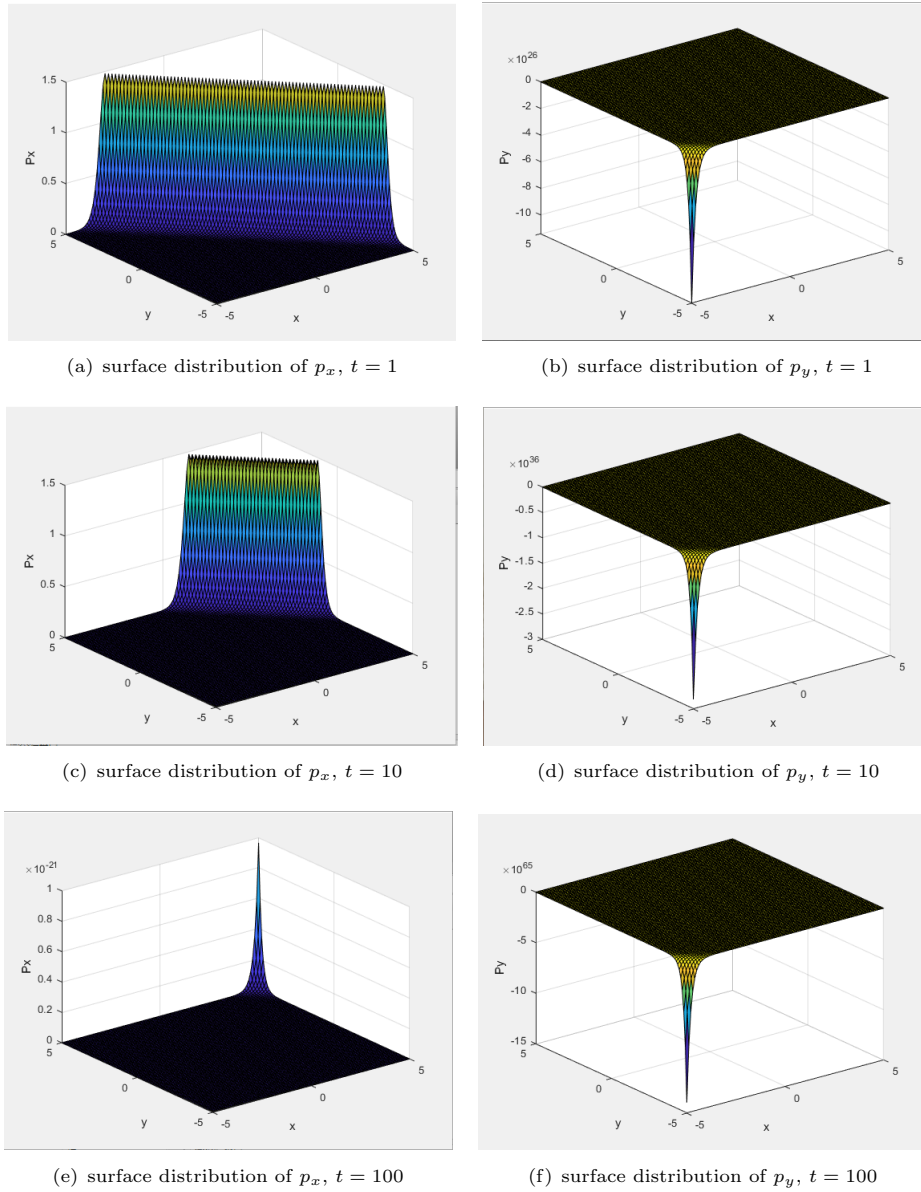


**Figure 3.** Case 1. The parameters are chosen as:  $\nu = 0.1$ ,  $l = 1$ ,  $C = -1$ ,  $C^* = -2$  and  $\alpha = \frac{1}{2}$ .

(i) Figs. 4, 5 and 6 are depicted to show the changes of the velocity field and the initial shape of spatial distribution of  $u_1$ ,  $u_2$  and  $p_x$ ,  $p_y$ . We can see that the vector  $\vec{u}$  whirls around origin ( $x = 0, y = 0$ ) only and the stream function  $\psi$  pictures a series of concentric circles merely within a certain circle. It is clear that the vectorial distribution of  $u_1$  and  $u_2$  are increasing as  $t$  increasing in Fig. 6.

(ii) Figs. 7 and 8 demonstrate the initial step shape of spatial distribution of  $u_1$ ,  $u_2$  and  $p_x$ ,  $p_y$  tend to be more and more gentle and their amplitude to be smaller with the increasing of  $t$ .

(iii) If we choose  $\nu = \frac{1}{Re}$ , where  $Re$  is Reynolds number, then we get that the change in  $\nu$  value may lead to change in shape of spatial distribution of  $u_1, u_2$  and  $p_x, p_y$ . With the increase in  $\nu$  value, their shape tend to be more and more gentle.

Choosing the fractional parameter  $\alpha = 1$  and  $\nu = \frac{1}{Re}$  in (4.3), we can get the same exact solution as in Ref. [23].

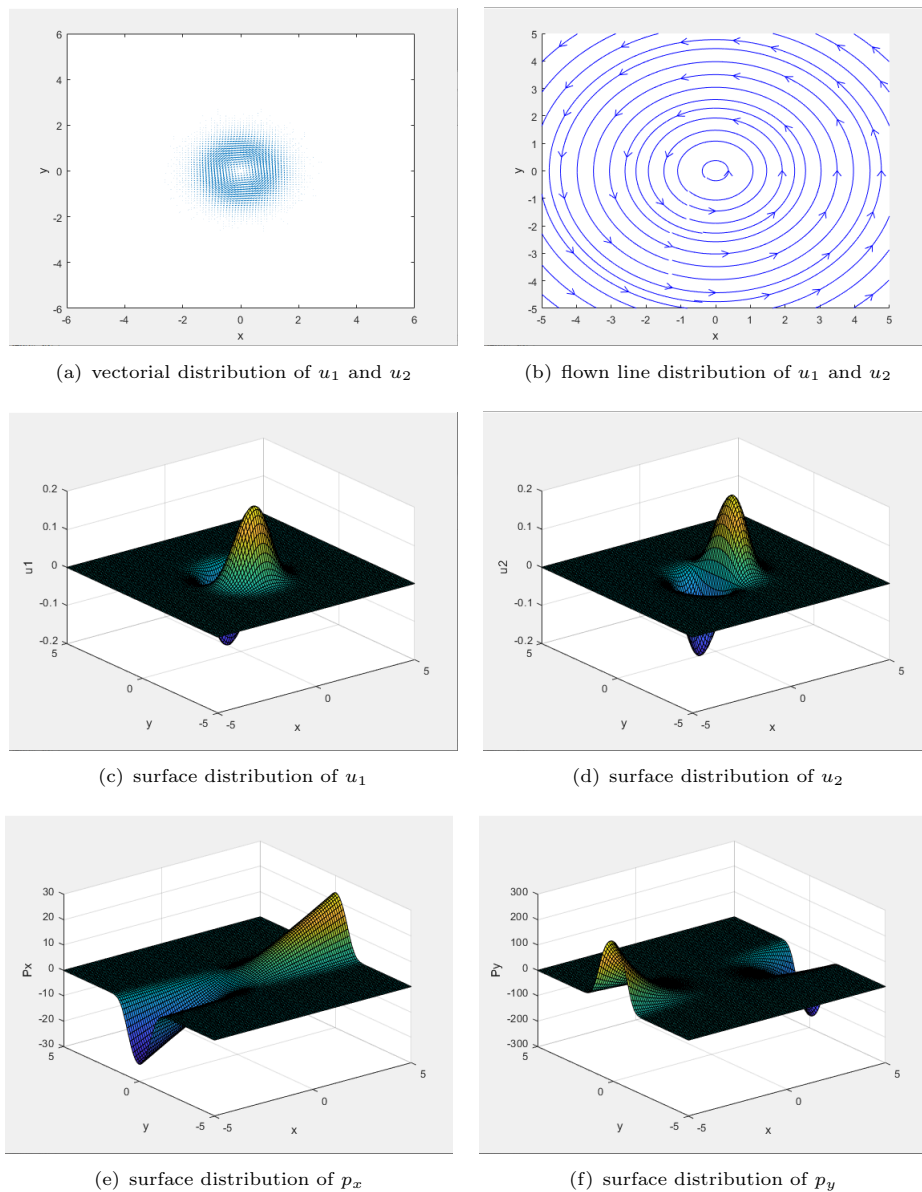


**Figure 4.** Case 2. The parameters are chosen as:  $\nu = 0.1, t = 1, x \times y \in [-5, 5] \times [-5, 5], a_0 = \exp(1)$  and  $\alpha = \frac{1}{2}$ .

**Case 3. An exact solution under action of a point source varying with time on infinity plane**

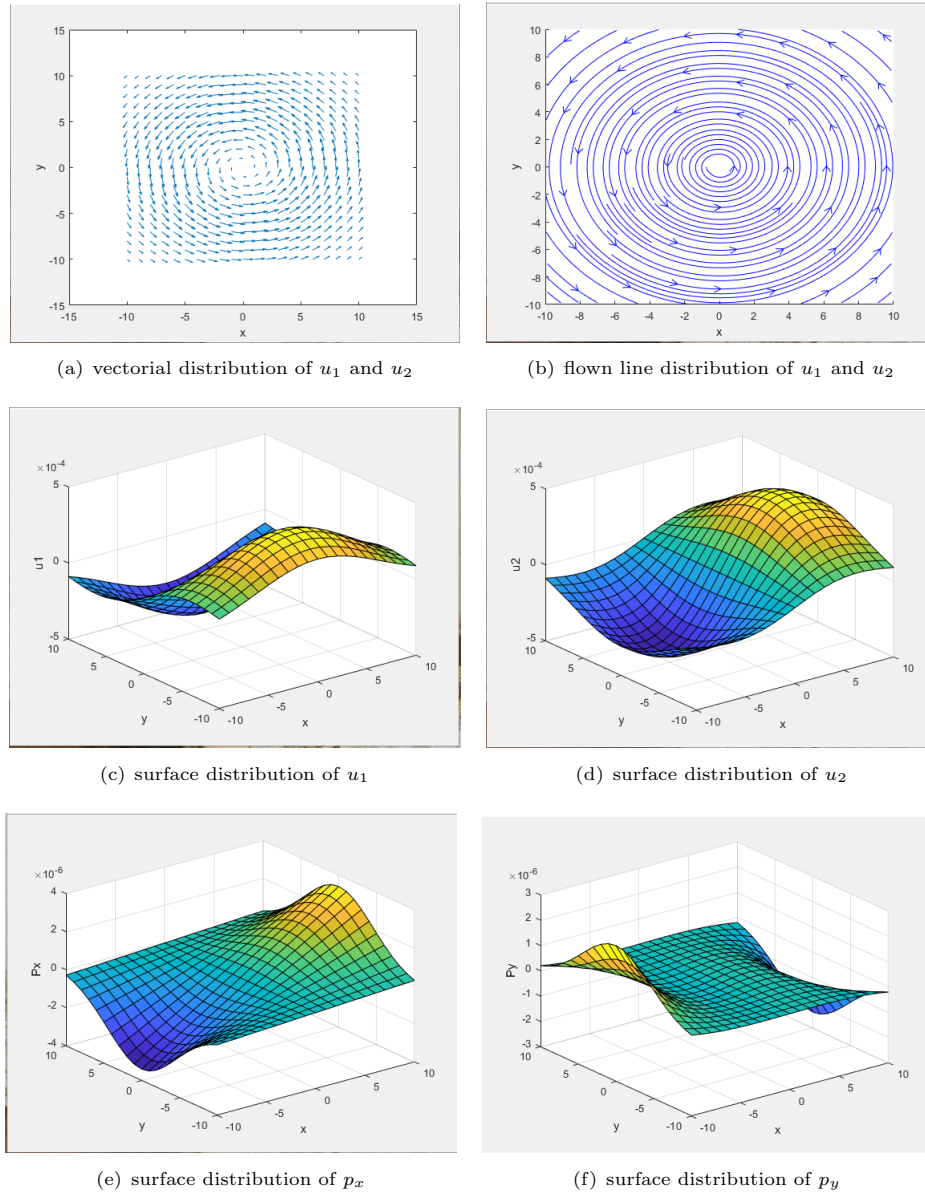


**Figure 5.** Case 2. The parameters are chosen as:  $\nu = 0.1$ ,  $t = 1$ ,  $x \times y \in [-10, 10] \times [-10, 10]$ ,  $a_0 = \exp(1)$  and  $\alpha = \frac{1}{2}$ .

Introducing an exact solution that satisfies (3.16) of the form

$$\begin{aligned}
 V(t, x, y) &= C_0 + V_1(t)H(\psi) \\
 &= C_0 + \exp\{C_0 \operatorname{sech}(C_1(t - C_2))\} \frac{1}{4\pi\nu t^\alpha} \exp\left\{-\frac{\alpha(x^2 + y^2)}{4\nu t^\alpha}\right\}, \quad (4.5)
 \end{aligned}$$

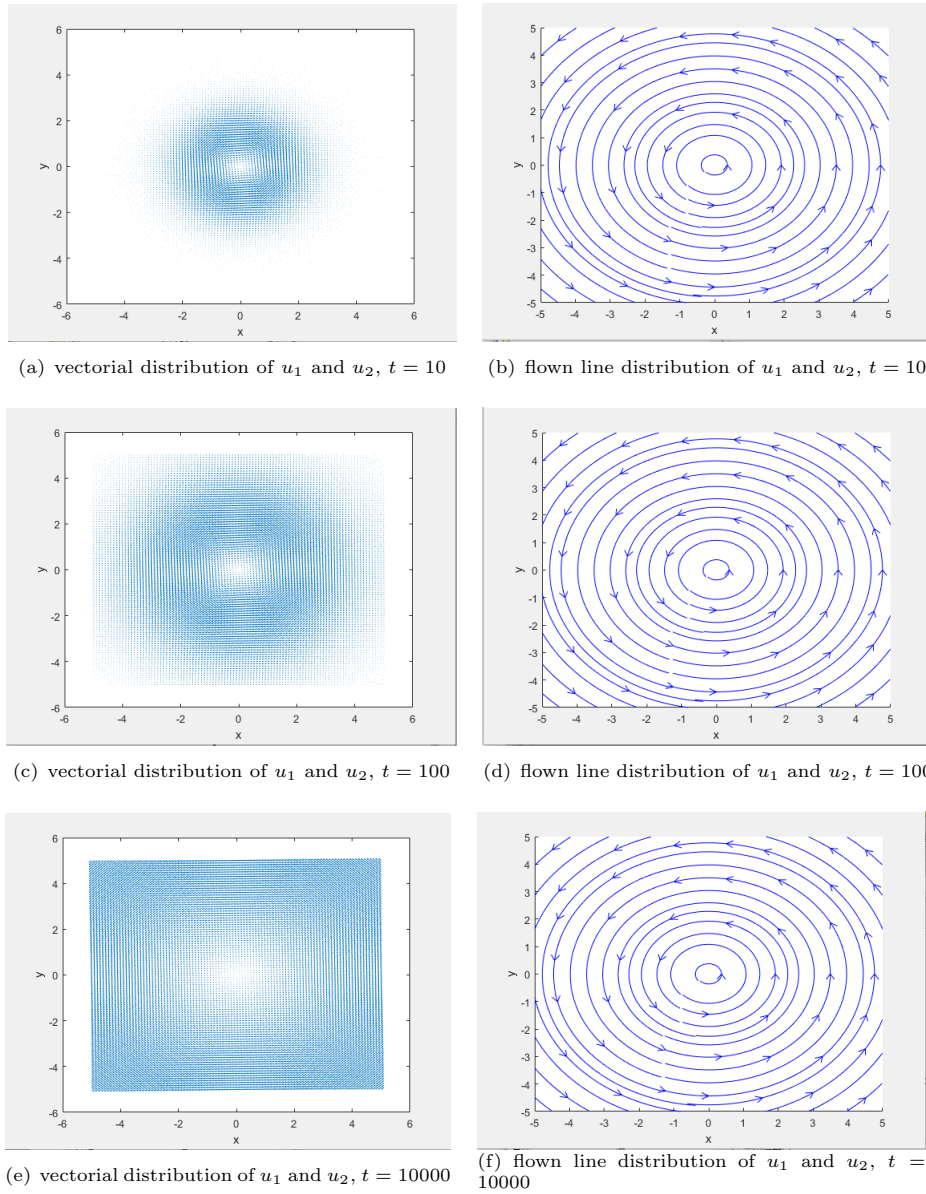


**Figure 6.** Case 2. The parameters are chosen as:  $\nu = 0.1$ ,  $t = 10000$ ,  $a_0 = \exp(1)$  and  $\alpha = \frac{1}{2}$ .

where  $V_1(t) = \exp\{C_0 \operatorname{sech}(C_1(t - C_2))\}$  and  $H(\psi) = \frac{1}{4\pi\nu t^\alpha} \exp\left\{-\frac{\alpha(x^2 + y^2)}{4\nu t^\alpha}\right\}$ .  
 Substituting (4.5) into (3.19) ~ (3.21), we have

$$\psi = -2\nu \ln\left(-\frac{C_0}{2\nu} - \frac{E_2}{8\pi\nu^2 t^\alpha}\right); \tag{4.6}$$

$$u_1 = \frac{-y\alpha E_2}{t^\alpha (4\pi C_0 \nu t^\alpha + E_2)}, u_2 = \frac{x\alpha E_2}{t^\alpha (4\pi C_0 \nu t^\alpha + E_2)}; \tag{4.7}$$

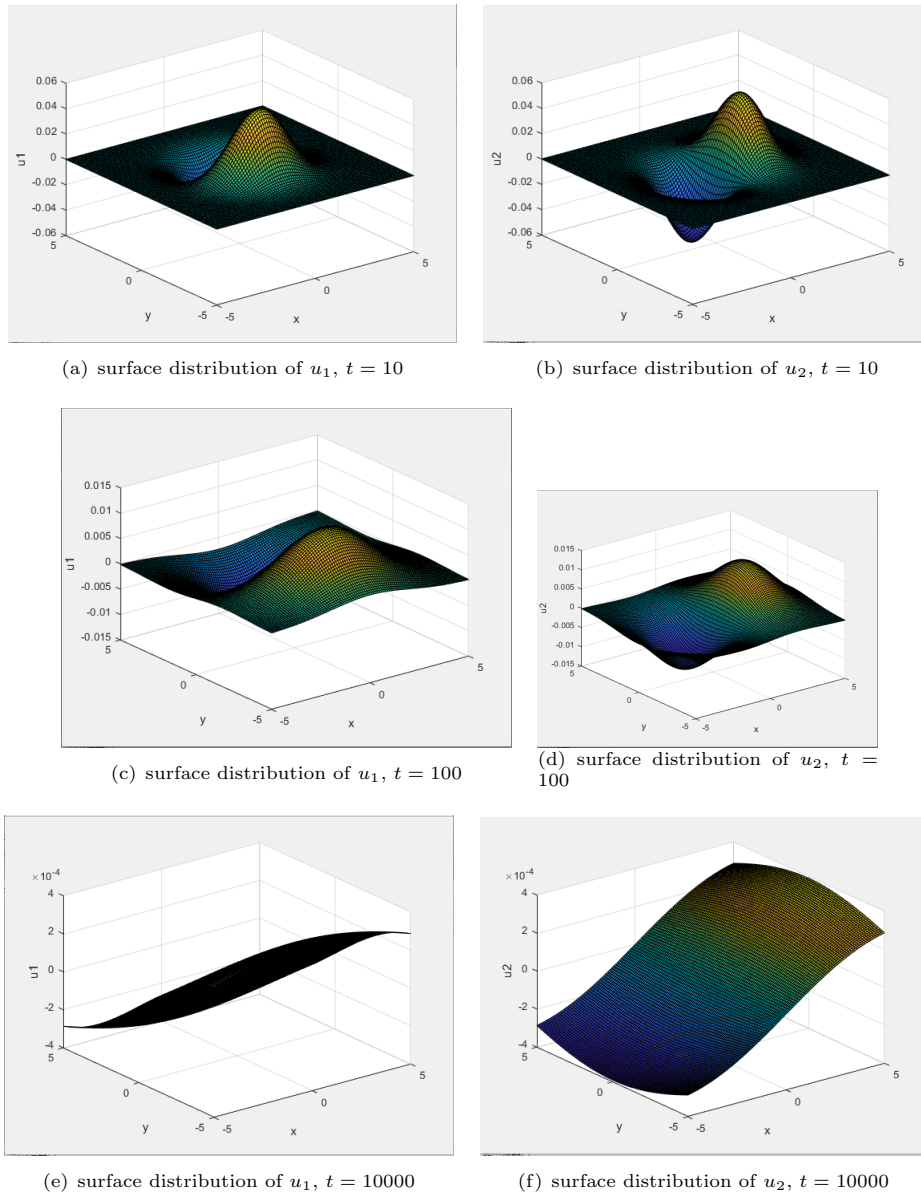


**Figure 7.** Case 2. The parameters are chosen as:  $\nu = 0.1$ ,  $t = 10000$ ,  $a_0 = \exp(1)$  and  $\alpha = \frac{1}{2}$ .

$$\begin{aligned}
 p_x = & \frac{\alpha^2 E_2^2 [2\pi C_0 \alpha y(x-y)^2 + 4\pi C_0 \nu t^\alpha (x-y) + E_2(x-y) + 4\pi C_0 \alpha x y^2]}{t^{2\alpha} (4\pi C_0 \nu t^\alpha + E_2)^3} \\
 & - \frac{4\pi C_0 C_1 \nu \alpha y t^{1-\alpha} E_2 \operatorname{sech}(C_1(t-C_2)) \tanh(C_1(t-C_2))}{(4\pi \nu t^\alpha + E_2)(4\pi C_0 \nu t^\alpha + E_2)}, \tag{4.8}
 \end{aligned}$$

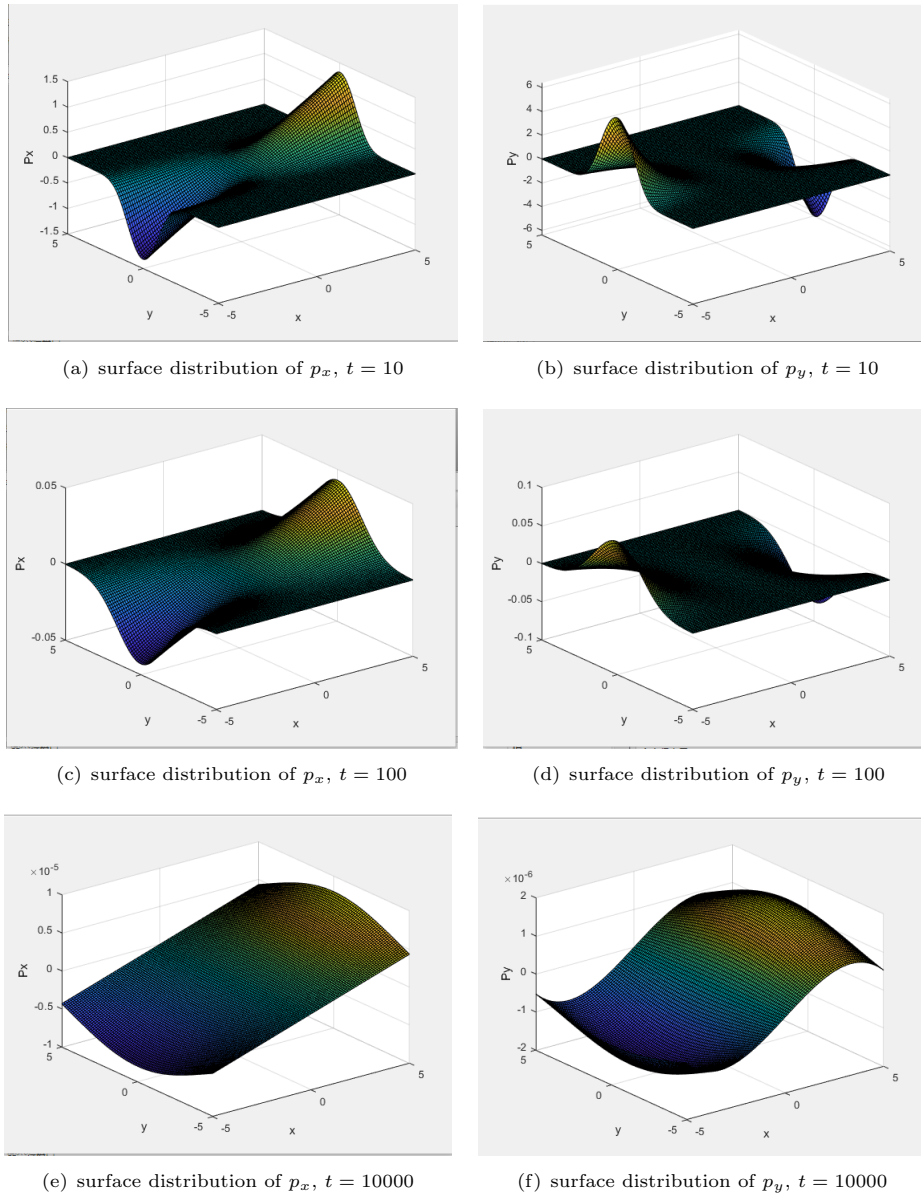


**Figure 8.** Case 2. The parameters are chosen as:  $\nu = 0.1$ ,  $t = 10000$ ,  $a_0 = \exp(1)$  and  $\alpha = \frac{1}{2}$ .

$$\begin{aligned}
 p_y = & \frac{\alpha^2 E_2^2 \left[ -2\pi C_0 \alpha x(x+y)^2 - 4\pi C_0 \nu t^\alpha (x+y) - E_2(x+y) + 4\pi C_0 \alpha x^2 y \right]}{t^{2\alpha} (4\pi C_0 \nu t^\alpha + E_2)^3} \\
 & + \frac{4\pi C_0 C_1 \nu \alpha x t^{1-\alpha} E_2 \operatorname{sech}(C_1(t - C_2)) \tanh(C_1(t - C_2))}{(4\pi \nu t^\alpha + E_2)(4\pi C_0 \nu t^\alpha + E_2)},
 \end{aligned}
 \tag{4.9}$$

where  $\psi$  is the stream function and  $E_2 = \exp \left\{ C_0 \operatorname{sech}(C_1(t - C_2)) - \frac{\alpha(x^2 + y^2)}{4\nu t^\alpha} \right\}$ . Substituting  $u_1$ ,  $u_2$  and  $p_x$ ,  $p_y$  into (3.1) ~ (3.2) and using the symbolic computation

method to calculate these variables, respectively, we can learn that the variables satisfy (3.1) ~ (3.2), thus the  $u_1, u_2$  and  $p_x, p_y$  in (4.6) ~ (4.9) constitute an exact solution of conformable 2D-TFNSEs.

The parameters are chosen as:  $\nu = 0.1, C_0 = 10.0, C_1 = 0.005, C_2 = 500.0$ , and  $\alpha = \frac{1}{4}$ . We can get some properties, as shown in Fig. 9. It is depicted to show the changes of the velocity field and the initial shape of spatial distribution of  $u_1, u_2$  and  $p_x, p_y$ , respectively. We can see that the vector  $\vec{u}$  whirls around origin ( $x = 0, y = 0$ ). Especially, the flown line distribution of  $\vec{u}$  in the region  $X \times Y \in [-5, 5] \times [-5, 5]$ , is more intensive than that in the rest of the region. The initial steep shape of spatial distribution of  $u_1, u_2$  and  $p_x, p_y$  tend to be more and more gentle and their amplitude to be smaller with the increase in time  $t$ .

Choosing the fractional parameter  $\alpha = 1, C_0 = 1$  and  $\nu = \frac{1}{Re}$  in (4.5), we can get the same exact solution as in Ref. [23].

#### Case 4. An exact solution with respect to initial boundary value problem in foursquare region

Introducing an exact solution that satisfies (3.8) of the form

$$W(t, x, y) = 1 + a_0 E_3 \frac{l^2}{\pi^2} \cos \frac{\pi x}{l} \cos \frac{\pi y}{l}, \quad (4.10)$$

where  $a_0$  is an initial boundary value, and  $l$  is a side length of foursquare region. Substituting (4.10) into (3.12) ~ (3.14), we have

$$\begin{aligned} \psi &= -2\nu \ln \left( -\frac{1}{2\nu} - \frac{a_0 l^2 E_3}{2\nu \pi^2} \cos \frac{\pi x}{l} \cos \frac{\pi y}{l} \right); \\ u_1 &= \frac{2\nu \pi a_0 l E_3 \cos \frac{\pi}{l} x \sin \frac{\pi}{l} y}{\pi^2 + a_0 l^2 E_3 \cos \frac{\pi}{l} x \cos \frac{\pi}{l} y}, u_2 = \frac{2\nu \pi a_0 l E_3 \sin \frac{\pi}{l} x \cos \frac{\pi}{l} y}{\pi^2 + a_0 l^2 E_3 \cos \frac{\pi}{l} x \cos \frac{\pi}{l} y}. \end{aligned} \quad (4.11)$$

Let

$$B(t, x, y) = \pi^2 + a_0 l^2 E_3 \cos \frac{\pi}{l} x \sin \frac{\pi}{l} y, \quad (4.12)$$

$$\begin{aligned} B_1(t, x, y) = \nu(u_{1xx} + u_{1yy}) &= -\frac{4\nu^2 \pi^3 a_0 E_3}{l B^3} \cdot \left( \pi^4 \cos \frac{\pi}{l} x \sin \frac{\pi}{l} y \right. \\ &\quad \left. + \pi^2 a_0 l^2 E_3 \sin^2 \frac{\pi}{l} x \sin \frac{\pi}{l} y \cos \frac{\pi}{l} y - a_0^2 l^4 E_3^2 \cos^3 \frac{\pi}{l} x \sin \frac{\pi}{l} y \right), \end{aligned} \quad (4.13)$$

$$\begin{aligned} B_2(t, x, y) = \nu(u_{2xx} + u_{2yy}) &= -\frac{4\nu^2 \pi^3 a_0 E_3}{l B^3} \cdot \left( \pi^4 \sin \frac{\pi}{l} x \cos \frac{\pi}{l} y \right. \\ &\quad \left. - \pi^2 a_0 l^2 E_3 \sin \frac{\pi}{l} x \sin \frac{\pi}{l} x \sin^2 \frac{\pi}{l} y - a_0^2 l^4 E_3^2 \cos^3 \frac{\pi}{l} y \sin \frac{\pi}{l} x \right), \end{aligned} \quad (4.14)$$

$$B_3(t, x, y) = \mathbf{D}_t^\alpha u_1 = \frac{-4\nu^2 \pi^5 a_0 E_3 \cos \frac{\pi}{l} x \sin \frac{\pi}{l} y}{l B^2}, \quad (4.15)$$

$$B_4(t, x, y) = \mathbf{D}_t^\alpha u_2 = \frac{-4\nu^2 \pi^5 a_0 E_3 \sin \frac{\pi}{l} x \cos \frac{\pi}{l} y}{l B^2}, \quad (4.16)$$

$$\begin{aligned} B_5(t, x, y) = u_1 u_{1x} + u_2 u_{1y} &= \frac{4\nu^2 \pi^3 a_0^2 l E_3^2}{B^3} \left( -\pi^2 \sin \frac{\pi}{l} x \cos \frac{\pi}{l} x \sin^2 \frac{\pi}{l} y \right. \\ &\quad \left. + \pi^2 \sin \frac{\pi}{l} x \cos \frac{\pi}{l} x \cos^2 \frac{\pi}{l} y + a_0 l^2 E_3 \sin \frac{\pi}{l} x \cos \frac{\pi}{l} y \cos^2 \frac{\pi}{l} x \right), \end{aligned} \quad (4.17)$$

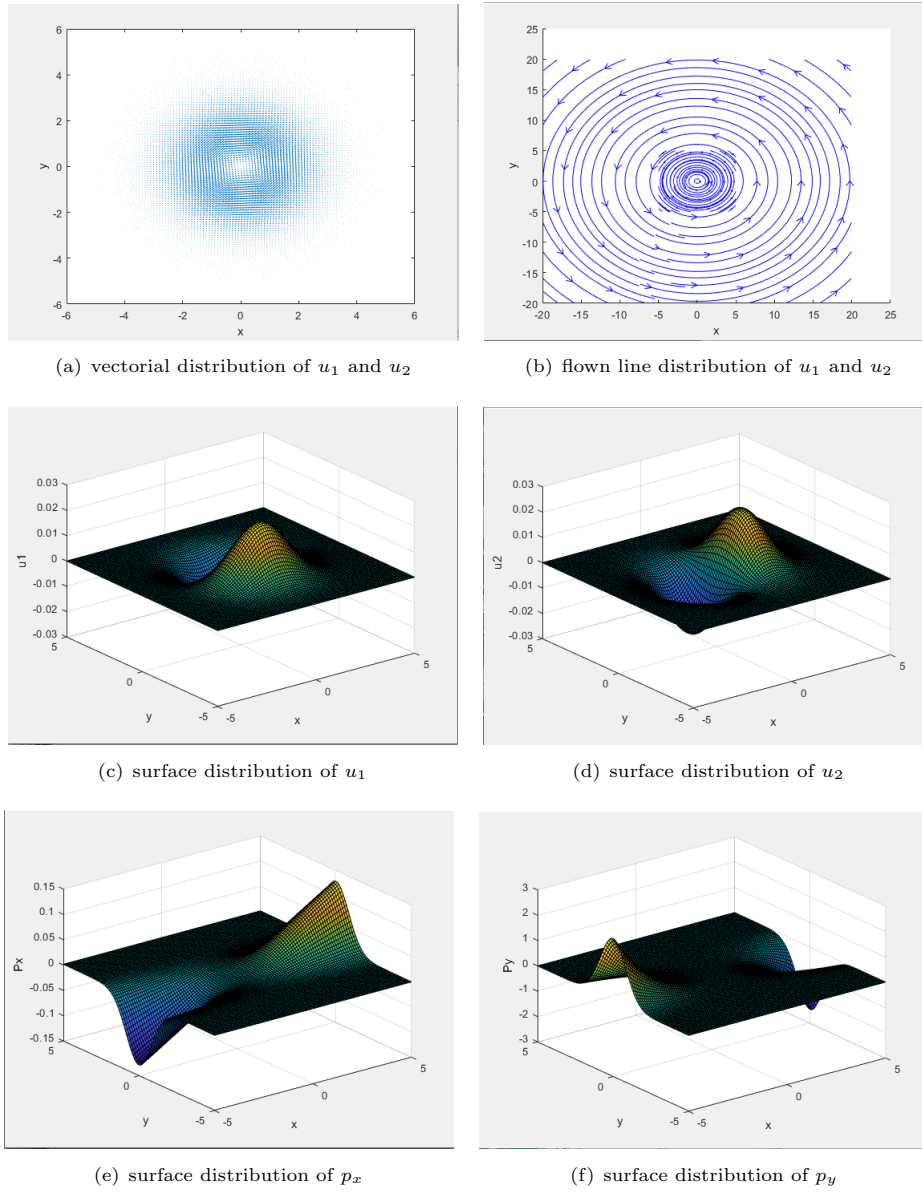


**Figure 9.** Case 3. The parameters are chosen as:  $\nu = 0.1$ ,  $C_0 = 10.0$ ,  $C_1 = 0.005$ ,  $C_2 = 500.0$ , and  $\alpha = \frac{1}{4}$ .

$$\begin{aligned}
 B_6(t, x, y) = u_1 u_{2x} + u_2 u_{1y} = & \frac{4\nu^2 \pi^3 a_0^2 l E_3^2}{B^3} \left( \pi^2 \cos^2 \frac{\pi}{l} x \sin \frac{\pi}{l} y \cos \frac{\pi}{l} y \right. \\
 & \left. + a_0 l^2 E_3 \cos \frac{\pi}{l} x \sin \frac{\pi}{l} y \cos^2 \frac{\pi}{l} y - \pi^2 \sin^2 \frac{\pi}{l} x \sin \frac{\pi}{l} y \cos \frac{\pi}{l} y \right), \quad (4.18)
 \end{aligned}$$

where  $E_3 = \exp \left\{ -\frac{2\nu\pi^2 t^\alpha}{\alpha l^2} \right\}$ . Then we get

$$\begin{aligned} p_x &= B_1(t, x, y) - B_3(t, x, y) - B_5(t, x, y), \\ p_y &= B_2(t, x, y) - B_4(t, x, y) - B_6(t, x, y). \end{aligned} \quad (4.19)$$

Following the procedure of the first case, we conclude that  $u_1$ ,  $u_2$  and  $p_x$ ,  $p_y$  in (4.4) constitute an exact solution of the conformable 2D-TFNSEs.

The exact solution for 2D-TFNSEs with respect to initial boundary value problem in foursquare region are obtained using Hopf-Cole transform. For a complete study and for possible comparisons, we present the parameters by making  $\nu = 0.01$ ,  $t = 10$ ,  $a_0 = \exp(3)$ ,  $\alpha = \frac{1}{4}$  and  $X \times Y \in [-5, 5] \times [-5, 5]$  or  $X \times Y \in [-20, 20] \times [-20, 20]$ . Some physical properties are found as shown in Fig. 10 and Fig. 11.

(i) Fig. 10 is depicted to show the changes of the vector field, the flown line distribution of  $u_1$  and  $u_2$ , and the shapes of spatial distribution of  $u_1$ ,  $u_2$  and  $p_x$ ,  $p_y$  when  $t = 10$ . It can be seen that the flown line distribution of  $\vec{u}$  pictures two families of hyperbolas.

(ii) In Fig. 11, it is clearly seen that  $u_1$  and  $u_2$  are the space periodic solutions, and their region of periodic is  $X \times Y \in [-20, 20] \times [-20, 20]$ .

(iii) If the parameters are chosen as Fig. 10, the shape of spatial distribution of  $u_1$ ,  $u_2$  and  $p_x$ ,  $p_y$  remain the same to the Fig. 10 with the increasing of  $t$ . These figures are omitted here for reasons of limited space.

## 5. Conclusions

The 2D-TFNSEs are considered in this paper for the first time. These new fluid models have a series of physical properties. Many conclusions are obtained as follows:

(i) Compared to 2D-NSEs, it is hard to solve the exact solutions of 2D-TFNSEs due to the time fractional derivative. With mass conservations (3.2) and the stream function  $\psi$  (3.3), 2D Hopf-Cole transformations are established by using the properties of conformable fractional operators and introducing a new variable  $W$  that satisfying the linear differential equations (3.8). If  $W$  can be found, it is possible to structure the corresponding exact solutions of TFNSEs. Next we must use symbolic computation method to test the obtained exact solutions according to point of Chiping Wu et al. in Refs. [24].

(ii) Exact solution in Case 1 provides that the velocity of the fluid tends to the constant value  $\vec{u} = (-1, 1)$  gradually as the fluid pressure  $p$  varying from strong to weak with  $t$  increasing. The flown line distribution of  $\vec{u}$  is a series of parallel lines. Especially the flown line distribution of  $\vec{u}$  in the region  $X \times Y \in [-20, 20] \times [-20, 20]$ , is more intensive than that in the rest of the region. It is seen clearly that the valued field of  $u_1$  is  $[-1, 0]$  and the surface distribution of  $u_1$  decrease gradually to  $u_1 = 1$  with the increasing of  $t$ . And then the valued field of  $u_2$  is  $[0, 1]$  and the surface distribution of  $u_2$  gradually decrease to  $u_2 = 1$  with the increase in time  $t$ . The surface distribution of  $p_x$  and  $p_y$  for three different values of  $t$ . It is clear that the surface distribution of  $p_x$  decreases from  $+\infty$  to  $p_x = 0$ , and the surface distribution of  $p_y$  increases from  $-\infty$  to  $p_y = 0$ .

(iii) Exact solution in Case 2 describes the gradual decreasing in vortex on infinity plane due to the influence of turbulent diffusion. Fig. 7 and Fig. 8

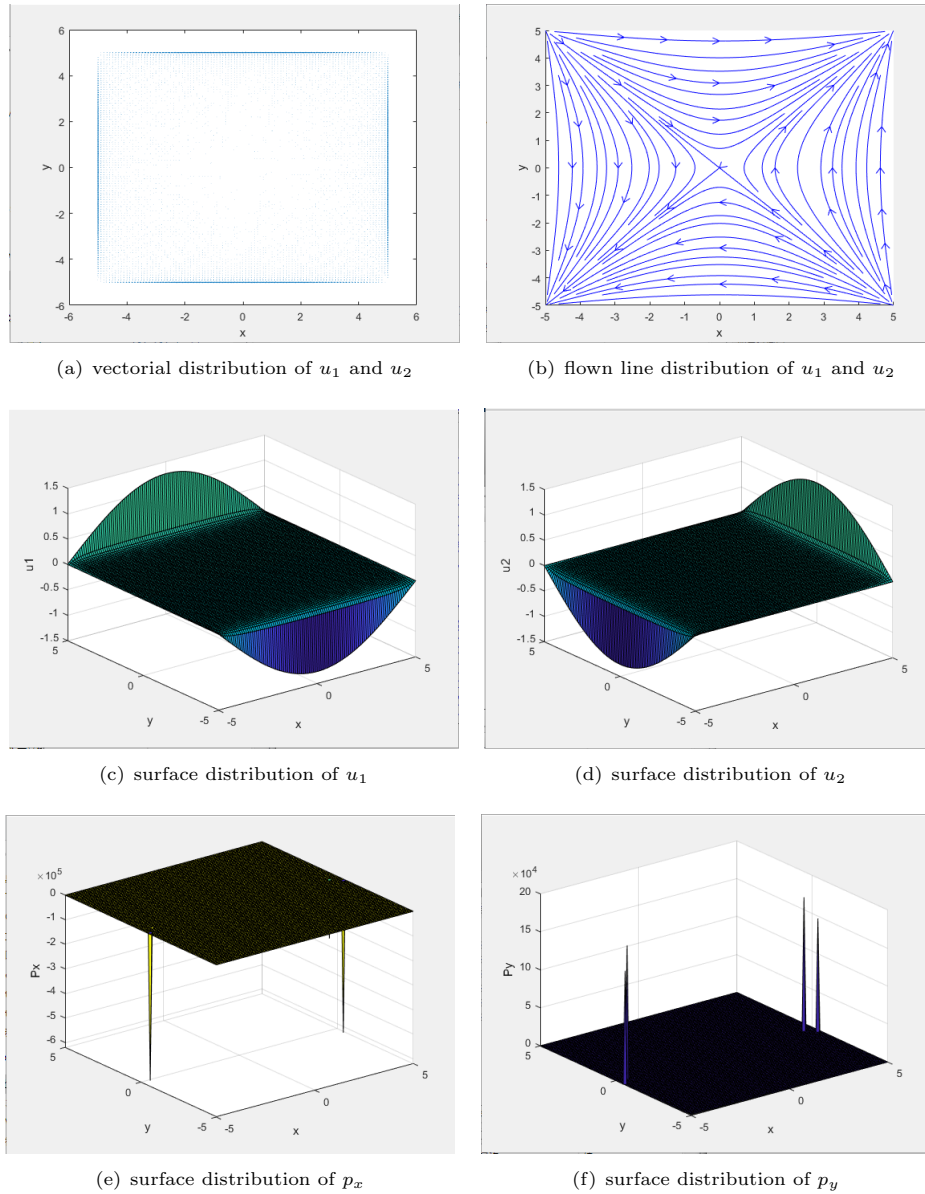


**Figure 10.** Case 4. The parameters are chosen as:  $\nu = 0.01$ ,  $t = 10$ ,  $a_0 = \exp(3)$ ,  $X \times Y \in [-5, 5] \times [-5, 5]$  and  $\alpha = \frac{1}{4}$ .

demonstrate the rotating vortex will gradually flatten out as the fluid pressure becoming weaker as time goes on. We can see that the vector  $\vec{u}$  whirls around origin ( $x = 0, y = 0$ ) only and stream function  $\psi$  pictures a series of concentric circles merely within a certain circle. It is clear that the vectorial distribution of  $u_1$  and  $u_2$  are increasing as  $t$  increasing. The initial step shape of spatial distribution of  $u_1, u_2$  and  $p_x, p_y$  tend to be more and more gentle and their amplitude to be smaller with the increasing of  $t$ . If we choose  $\nu = \frac{1}{Re}$ , then we get that the change

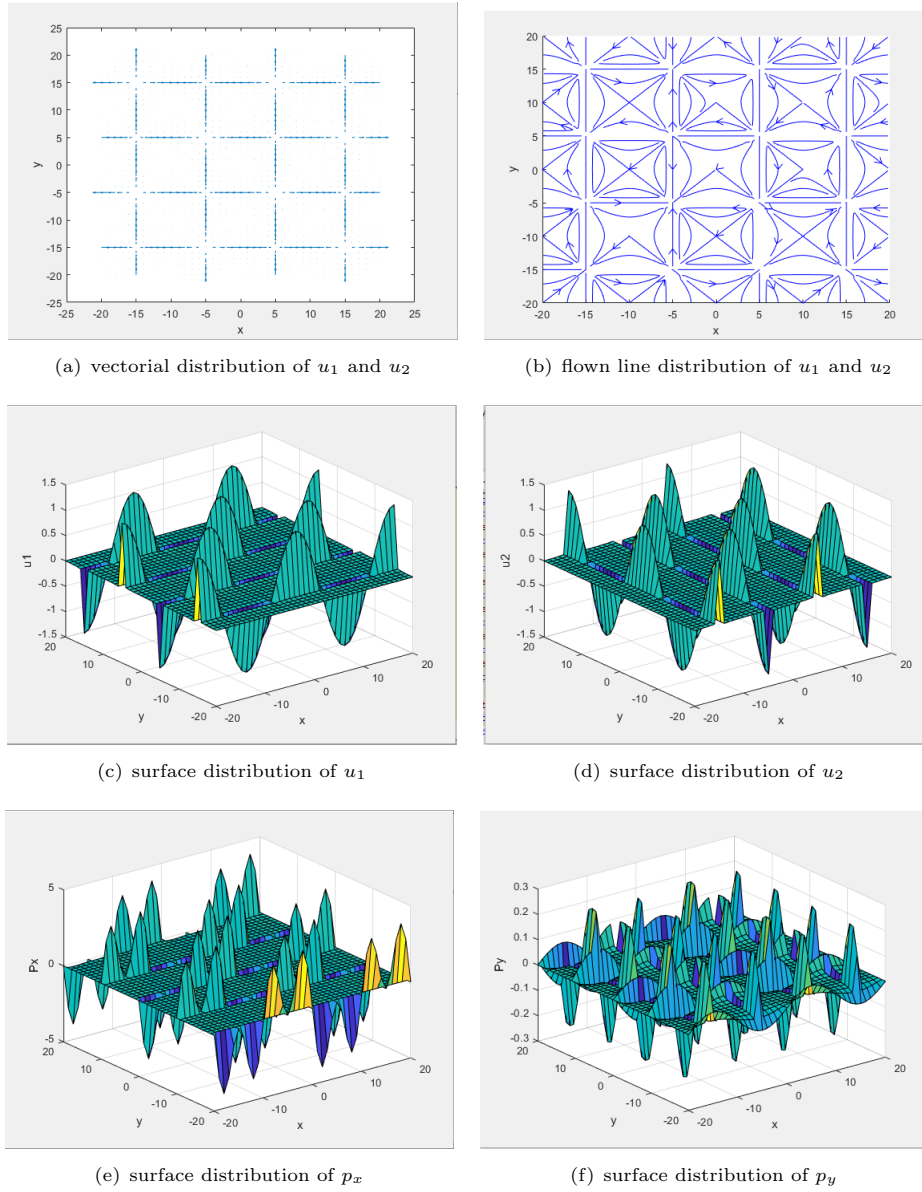


**Figure 11.** Case 4. The parameters are chosen as:  $\nu = 0.01$ ,  $t = 10$ ,  $a_0 = \exp(3)$ ,  $X \times Y \in [-20, 20] \times [-20, 20]$  and  $\alpha = \frac{1}{4}$ .

in  $\nu$  value may lead to change in shape of spatial distribution of  $u_1$ ,  $u_2$  and  $p_x$ ,  $p_y$ . With the increasing of  $\nu$  value, their shape tend to be more and more gentle. In other words, the higher of the density becomes, the gentler of fluid motion.

(iv) Exact solution in Case 3 provides a description of 2D vortex moving from weak to strong and then to weak on infinity plane. The vector  $\vec{u}$  in this case whirls around origin ( $x = 0, y = 0$ ), too. Especially, the flown line distribution of  $\vec{u}$  in the region  $X \times Y \in [-5, 5] \times [-5, 5]$ , is more intensive than that in the rest of the

region. The initial steep shape of spatial distribution of  $u_1$ ,  $u_2$  and  $p_x$ ,  $p_y$  tend to be more and more gentle and their amplitude to be smaller with the increasing of  $t$ .

(v) The exact solution in Case 4 describes the circumfluence obvious characteristic of periodic changes within foursquare region because of the influence of turbulent diffusion, see Fig. 11. We can see that the flown line distribution of  $\vec{u}$  pictures two families of hyperbolas. It is clearly seen that  $u_1$  and  $u_2$  are the space periodic solutions, and their region of periodic is  $X \times Y \in [-5, 5] \times [-5, 5]$ . If the parameters are chosen as Fig. 10, the shape of spatial distribution of  $u_1$ ,  $u_2$  and  $p_x$ ,  $p_y$  remain the same to the Fig. 10 with the increasing of  $t$ .

**Acknowledgements.** The authors are grateful to the anonymous referees for their useful suggestions which improve the contents of this article.

## References

- [1] T. Abdeljawad, *On conformable fractional calculus*, Comput. Appl. Math., 2015, 279, 57–66.
- [2] A. Atangana, D. Baleanu and A. Alsaedi, *New properties of conformable derivative*, Open Math., 2015, 13, 889–898.
- [3] Charles-Henri Bruneau and Sandra Tancogne *Far field boundary conditions for incompressible flows computation*, J. Appl. Anal. Comput., 2018, 8:3, 690-709.
- [4] W. Chung, *Fractional Newton mechanics with conformable fractional derivative*, Comput. Appl. Math., 2015, 290, 150–158.
- [5] K. Diethelm, *The analysis of fractional differential equations*, Springer, Berlin, 2010.
- [6] Y. He and W. Sun, *Stability and convergence of the Crank-Nicolson/Adams-Bashforth scheme for the time-dependent Navier-Stokes equations*, 2007, SIAM J. Numer. Anal., 45(2), 837–869.
- [7] R. Ingram, *A new linearly extrapolated Crank-Nicolson time-stepping scheme for the Navier-Stokes equations*, Math. Comp., 2013, 82(284), 1953–1973.
- [8] S. Kaya and B. Rivière, *A discontinuous subgrid eddy viscosity method for the time-dependent Navier-Stokes equations*, SIAM J. Numer. Anal., 2005, 43(4), 1572–1595.
- [9] R. Khalil, M. Alhorani, A. Yousef and M. Sababheh, *A new definition of fractional derivative*, Comput. Appl. Math., 2014, 65–70.
- [10] H. C. Ku and D. Hatzivramidis, *Solutions of the two-dimensional Navier-Stokes equations by Chebyshev expansion methods*, Computer & Fluids, 1985, 13(1), 99–113.
- [11] L. Peng, A. Debbouche and Y. Zhou, *Existence and approximations of solutions for time-fractional Navier-Stokes equations*, Math. Meth. Appl. Sci., 2018, 4, 1–12.
- [12] I. Podlubny, *Fractional differential equations*, Academic Press, San Diego, 1999.
- [13] G. Profilo, G. Soliani and C. Tebaldi, *Some exact solutions of the two-dimensional Navier-Stokes equations*, Int. J. Engng Sci., 1998, 36(4), 459–471.

- [14] A. A. Ragab, K. M. Hemida, M. S. Mohamed and M. A. Abd El Salam, *Solution of time fractional Navier-Stokes equation by using Homotopy analysis method*, Gen. Math. Notes, 2012, 13(2), 13–21.
- [15] T. Saitoh, *A numerical method for two-dimensional Navier-Stokes equation by multi-point finite differences*, International J. Numer. Meth. Engin., 1977, 11, 1439–1454.
- [16] L. Shan and Y. Hou, *A fully discrete stabilized finite element method for the time-dependent Navier-Stokes equations*, Appl. Math. Comput., 2009, 215(1), 85–99.
- [17] A. Shirikyan, *Analyticity of solutions for randomly forced two-dimensional Navier-Stokes equations*, Russian Math. Surveys, 2002, 54(4), 785–799.
- [18] R. M. Terrill, *An exact solution for flow in a porous pipe*, Appl. Math. Phys., 1982, 33(4), 547–552.
- [19] B. Tian and Y. Gao, *Spherical Kadomtsev-Petviashvili equation and nebulons for dustion-acoustic waves with symbolic computation*, Physics Letters A, 2005, 340, 243–250.
- [20] B. Tian and Y. Gao, *On the solitonic structures of the cylindrical dust-acoustic and dust-ion-acoustic waves with symbolic computation*, Physics Letters A, 2005, 340, 449–455.
- [21] D. J. Torres and E. A. Coutsias, *Pseudospectral solution of the two-dimensional Navier-Stokes equations in a disk*, SIAM J. Sci. Comput., 1999, 21(1), 378–403.
- [22] S. Tsangaris, D. Kondaxakis and N. W. Vlachakis, *Exact solution of the Navier-Stokes equations for the pulsating Dean flow in a channel with porous walls*, International J. Engin. Sci., 2006, 44, 1498–1509.
- [23] C. Wu, Z. Ji, Y. Zhang, J. Hao and X. Jin, *Some new exact solutions for the two-dimensional Navier-Stokes equations*, Physics Letters A, 2007, 371, 438–452.
- [24] C. Y. Wang, *Flow due to a stretching boundary with partial slip-an exact solution of the Navier-Stokes equations*, Chemical Engineering Science, 2002, 57, 3745–3747.
- [25] Z. Zhang, X. Ouyang and X. Yang, *Refined a priori estimates for the axisymmetric Navier-Stokes equations*, J. Appl. Anal. Comput., 2017, 7, 554–558.
- [26] Yuqing Zhang, Yuan Li and Rong An, *Two-level iteration penalty and variational multiscale method for steady incompressible flows*, J. Appl. Anal. Comput., 2016, 6, 607–627.
- [27] Z. Zhao, *Exact solutions of a class of second-order nonlocal boundary value problems and applications*, Appl. Math. Comput., 2009, 215(5), 1926–1936.
- [28] D. Zhao and M. Luo, *General conformable fractional derivative and its physical interpretation*, Calcolo, 2017. [https://DOI 10.1007/s10092-017-0213-8](https://doi.org/10.1007/s10092-017-0213-8).
- [29] Y. Zhou and L. Peng, *Weak solutions of the time fractional Navier-Stokes equations and optimal control*, Comput. Math. Appl., 2017, 73(6), 1016–1027.
- [30] G. Zou, Y. Zhou, B. Ahmad and A. Alsaedi, *Finite difference/element method for time-fractional Navier-Stokes equations*, Appl. Comput. Math., 2018, arXiv:1802.09779v1[math. NA].